

Proton distributions in dp dielectron production within Regge theory
A.P.Jerusalimov, G.I.Lykasov

JINR, Dubna, Moscow region, 141980, Russia

Abstract

The processes of dielectron production in deuteron-proton collisions at intermediate incident deuteron beam energies are analyzed in the spectator model within the one-pion exchange reggeized approach. We focus mainly on the momentum and angle distributions of the proton-spectator and the proton emitted in quasi-free NN processes at small angles in the laboratory frame. It is shown that the inclusion of many channels in quasi-free NN interaction allows us to describe the HADES data quite satisfactorily at incident deuteron kinetic energies of about 2.5 GeV.

1. Introduction

As it is well known, the Regge theory [1] is well applied in the analysis of inclusive hadron production in nucleon-nucleon and pion-nucleon collisions at high energies and not large transfers. For analysis of the exclusive production of one or two pions in NN or πN interactions the one-pion exchange reggeized (OPER) model was suggested [2]. For example, recently the OPER was successfully applied [3, 4] to describe the experimental data on two-pion production in np collisions at incident kinetic energies E_{kin} of about 1-5 GeV [3, 5, 6, 7] and the HADES data at $E_{kin} = 1.25$ GeV [4]. One of the most interesting goals in the HADES program is the study of e^+e^- -pair production in np interactions. But there are no pure narrow neutron beams in the world. Thus, this process can only be studied using the dp or pd -interactions.

The HADES [8] (**H**igh **A**acceptance **D**i-**E**lectron **S**pectrometer) is designed at GSI (Darmstead, Germany) and operated at the SIS synchrotron at nuclear (A) beam energies of about 1-2 A GeV. It is a magnetic spectrometer capable of registering both hadrons (p, K- and π -mesons) and e^+/e^- pairs within the range of polar angles from 17° up to 85° and exhibits a nearly full azimuth coverage. The main goal of the HADES experiments is the study of hadron properties inside the hot and dense nuclear medium via their di-electron decays. One specific aspect of heavy-ion reactions in the 1-2 AGeV range is the important role of baryonic resonances produced, that propagate due to the long lifetime of the dense hadronic

matter phase. A detailed description of resonance excitation and its coupling to the pseudo-scalar and vector mesons is significant for interpretation of the di-electron spectra measured by HADES.

The broad experimental program includes the study of e^+e^- -pair production in nucleus-nucleus collisions, elementary reactions (pp , np , πp) as well as pA , πA collisions with the emphasis on properties of vector mesons at finite baryonic densities.

2. Calculation procedure

2.1 Spectator mechanism for dielectron production in the dp reaction

If the proton is emitted in the forward direction, i.e., at small angles relative to the beam in the reaction $dp \rightarrow pe^+e^-X$, then one can use the so-called spectator diagram to analyze spectra of the hadrons and dielectrons produced. Here the system X can contain two nucleons and a few pions. This diagram is presented in Fig. 1, where p_s is the spectator proton. In this case the dielectron pair is produced in the quasi-free $np \rightarrow e^+e^-X$ reaction. In principle, the neutron can also be treated as a spectator, (n_s), then dielectrons are produced in the quasi-free $pp \rightarrow e^+e^-X$ process. To resolve the spectator neutron problem the HADES set-up

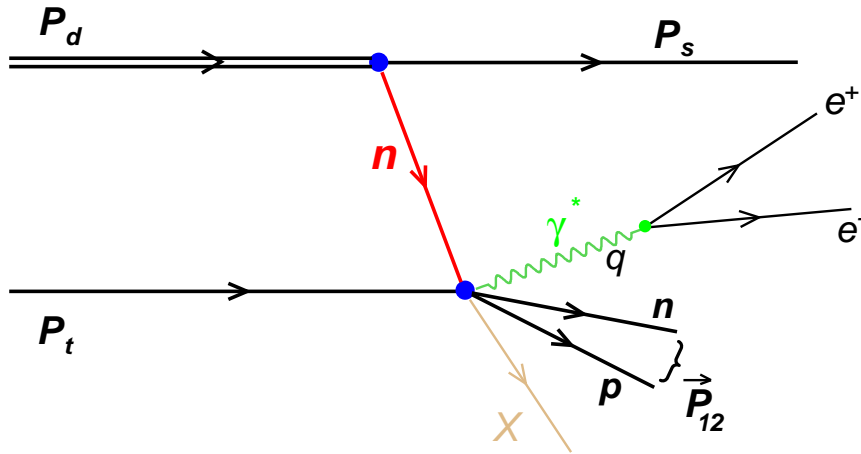


Figure 1: The spectator diagram for the process $dp \rightarrow p_s e + e - X$. Here P_d , P_t , P_s and \vec{P}_{12} stand for the momenta of the deuteron, proton-target, proton-spectator and of the three-momentum of the final proton (p) and neutron (n), respectively; X represents one or two pions.

[8] was upgraded with the **F**orward scintillator hodoscope **W**all (**FW**) [9, 10] to select quasi-free $n-p$ reactions by detecting fast spectator protons from the deuteron break-up. The **FW** was located 7 m downstream from the proton target covering

polar angles between 0.3° and 7.0° and provided the time-of-flight information that permitted to reconstruct the proton-spectator momentum.

The **FW** can register not only the proton-spectator, but also other charged particles (mainly secondary protons).

To eliminate dilepton pairs produced by γ conversion in the detector material the e^+e^- -pairs were selected at angles $\Theta_{ee}^{LAB} > 9^\circ$.

The spectra of nucleons and of dielectron pairs produced in the dp reaction were calculated by MC simulation inputting the nucleon momentum distribution inside the deuteron and the differential cross section of the processes $NN \rightarrow NNXe^+e^-$. As for the deuteron wave function (DWF), the CD-Bonn DWF [11] was used. The differential cross section of the $NN \rightarrow e^+e^-X$ reaction was calculated within the one-pion exchange reggeized (OPER) model [2].

2..2 OPER

The OPER model is based on the method of complex momenta [1]. In Fig. 2 the one-Reggeon R exchange graph in the t channel of the binary process $a + b \rightarrow c + d$ is presented. The virtual state R has quantum numbers of a particle or a resonance

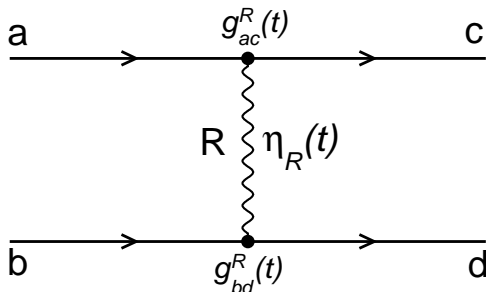


Figure 2: Diagram of the process $a + b \rightarrow c + d$

with a certain spin and orbital momentum in the complex space, which corresponds to a Regge trajectory $\alpha_R(t)$ that is a function of the transfer t . The amplitude of binary processes $a + b \rightarrow c + d$ presented in Fig. 2 is given by the following [1]:

$$T_R(s, t) = i8\pi s_0 g_{ac}^R(t) \eta_R(t) \left(\frac{ss_0}{m_c^2 m_d^2} \right)^{\alpha_R(t)} g_{bd}^R(t). \quad (1)$$

Here s is the initial energy squared, s_0 is the energy scale factor, which is usually chosen to be about 1 GeV^2 , m_c, m_d are the masses of the produced hadrons c and d , respectively; $g_{ac}^R(t)$ ($g_{bd}^R(t)$) is the vertex function or the so-called Regge form factor depending on the transfer t , which is usually parametrized in the simple exponential form $g_{ac}^R(t) = g_{ac}^R(t=0) \exp(-R^2 |t|)$, where the parameter R is called the Regge radius, $\eta_R(t)$ is the signature factor, determined as follows:

$$\eta_R(t) = - \frac{\sigma + \exp(-i\pi\alpha_R(t))}{\sin[\pi\alpha_R(t)]}, \quad (2)$$

where $\sigma = \pm 1$ is the signature value. If $\sigma = +1$, then $\eta_R(t) = i - ctg(\pi\alpha_R(t)/2)$ and $\eta_R(t) = i - tg(\pi\alpha_R(t)/2)$ at $\sigma = -1$.

The pion Regge trajectory, which is a linear function of t , can be expanded in the following approximate form, see for example [12, 13]:

$$\alpha_R(t) = \alpha_R(t=0) + \alpha'_R(t=0) \cdot t, \quad (3)$$

where $\alpha_R(t=0)$ is the intercept of the Regge trajectory, $\alpha'_R(t=0)$ is its derivative at $t=0$. The diagrams of the one-pion exchange reggeized for the reaction $np \rightarrow$

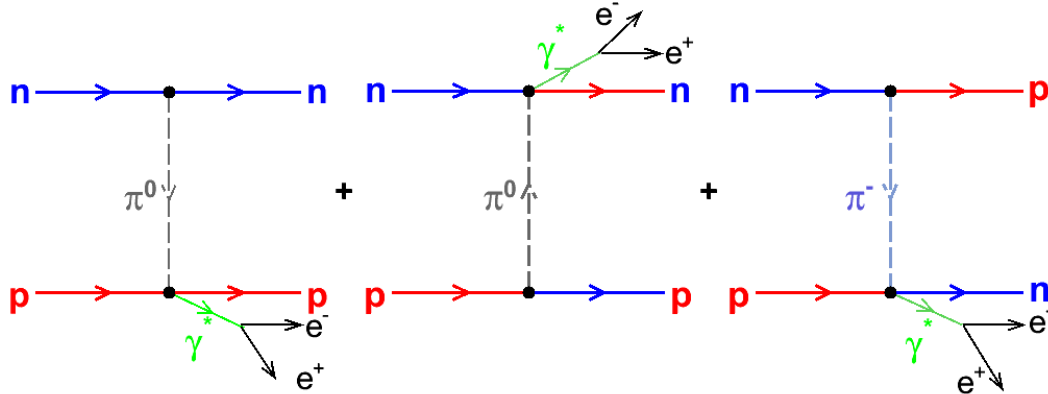


Figure 3: The one-pion exchange reggeized for the reaction $np \rightarrow \gamma * np \rightarrow e^+ e^- np$.

$\gamma * np \rightarrow e^+ e^- np$ are presented in Fig. 3. The amplitude of this process within the OPER can be presented in the following form:

$$T_{NN \rightarrow NN \gamma^* \rightarrow NN e^+ e^-} = G_{\pi N} \nu(\bar{p}'_N) \Gamma_{\pi N} u(p_N) F_{\pi N} f_{\pi N \rightarrow \gamma^* N \rightarrow e^+ e^- N} \quad (4)$$

where

$$F_{\pi N} = \exp[(R_1^2 + \alpha'_\pi \ln(s(\mu^2 + k_{\gamma^* \perp}^2)/(s_0 s_1)))(t - \mu^2)] \quad (5)$$

Here, the following notation is introduced: $\Gamma_{\pi N} = \gamma_5 q_m \gamma^m$ or $\Gamma_{\pi N} = \gamma_5$; $s = (p_n + p_p)^2$; $s_1 = (p_\pi + p_p)^2$; $s_2 = (p_n + k_{\gamma^*})^2$; $t = (p'_N - p_p)^2$; p_n, p_p, p_π are the four-momenta of the initial neutron, proton and exchange pion, respectively; p_N, p'_N, k_{γ^*} are the four-momenta of the final nucleon and virtual time-like photon decaying into a $e^+ e^-$ pair.

The slope of the pion trajectory $\alpha'_\pi = 0.7$ is well-known, see, for example, [2]. The parameter value $R_1^2 = 3.3 \text{ GeV}^{-2}$ is chosen from the best description of many observables of dielectron production in the quasi-free np interaction presented below. In the general case we calculated the amplitude of the process $NN \rightarrow \gamma * np \rightarrow e^+ e^- X$, where X can stand for two nucleons and one or two pions. In the next subsection we present the different channels of dielectron production in the NN interaction.

2..3 Different channels of dielectron production in quasi-free NN interactions

The following reactions were taken into account to describe the production of e^+e^- -pairs (p_s denotes the spectator proton and n_s is the spectator neutron):

$dp \rightarrow p_s + (np \rightarrow e^+e^- + X)$:

$$\begin{aligned}
np &\rightarrow npe^+e^-, \\
np &\rightarrow np\pi^0, \quad \pi^0 \rightarrow e^+e^-\gamma \\
np &\rightarrow np\pi^0\pi^0, \quad \pi^0 \rightarrow e^+e^-\gamma \\
np &\rightarrow \Delta^0 p, \quad \Delta^0 \rightarrow ne^+e^- \\
np &\rightarrow \Delta^+ n, \quad \Delta^+ \rightarrow pe^+e^- \\
np &\rightarrow \Delta^0 N\pi, \quad \Delta^0 \rightarrow ne^+e^-, \quad N\pi = n\pi^+ \text{ \& \ } p\pi^0 \\
np &\rightarrow \Delta^+ N\pi, \quad \Delta^+ \rightarrow pe^+e^-, \quad N\pi = n\pi^0 \text{ \& \ } p\pi^- \\
np &\rightarrow np\eta^0, \quad \eta^0 \rightarrow e^+e^-\gamma \\
np &\rightarrow np\rho^0, \quad \rho^0 \rightarrow e^+e^-
\end{aligned}$$

$dp \rightarrow n_s + (pp \rightarrow e^+e^- + X)$:

$$\begin{aligned}
pp &\rightarrow pp\pi^0, \quad \pi^0 \rightarrow e^+e^-\gamma \\
pp &\rightarrow pp\pi^0\pi^0, \quad \pi^0 \rightarrow e^+e^-\gamma \\
pp &\rightarrow \Delta^+ p, \quad \Delta^+ \rightarrow pe^+e^- \\
pp &\rightarrow \Delta^0 p\pi^+, \quad \Delta^0 \rightarrow ne^+e^-, \\
pp &\rightarrow \Delta^+ N\pi, \quad \Delta^+ \rightarrow pe^+e^-, \quad N\pi = p\pi^0 \text{ \& \ } n\pi^+
\end{aligned}$$

The rates of these processes to the total yield of the $np \rightarrow npe^+e^-X$ at the effective dielectron mass $M_{ee} < 0.140\text{GeV}/c^2$ are presented in Table 1.

Table 1: $M_{ee} < 0.140\text{GeV}/c^2$

Reaction	$0.5^\circ < \Theta < 2.0^\circ$	$2.0^\circ < \Theta < 4.0^\circ$	$4.0^\circ < \Theta < 6.0^\circ$
$np \rightarrow np\pi^0$	0.826	0.759	0.533
$np \rightarrow np\pi^0\pi^0$	0.036	0.064	0.063
$np \rightarrow npe^+e^-$	0.041	0.005	0.004
$np \rightarrow \Delta N$	0.001	0.001	0.001
$np \rightarrow \Delta N\pi$	0.025	0.013	0.011
$np \rightarrow np\eta^0$	0.017	0.008	0.007
$pp \rightarrow pp\pi^0$	0.045	0.118	0.212
$pp \rightarrow pp\pi^0\pi^0$	0.002	0.003	0.005
$pp \rightarrow \Delta^+ p$	<0.001	0.001	0.004
$pp \rightarrow \Delta^+ N\pi$	0.007	0.028	0.160

One can see from Table 1 that the main contribution to dielectron production in the np interaction at $M_{ee} < 0.14 \text{ GeV}/c^2$ comes from the channel $np \rightarrow np\pi^0$ with

the subsequent $\pi^0 \rightarrow e^+e^-\gamma$ decay. The decay amplitudes of π^0, ρ^0, η^0 -mesons and the Δ -isobar were calculated using the PLUTO model [14, 15, 16].

The rates of these processes to the total yield of the $np \rightarrow npe^+e^-X$ at the effective dielectron mass $M_{ee} > 0.140\text{GeV}/c^2$ are presented in Table 2. One can see

Table 2: $M_{ee} > 0.140\text{GeV}/c^2$

Reaction	$0.5^\circ < \Theta < 2.0^\circ$	$2.0^\circ < \Theta < 4.0^\circ$	$4.0^\circ < \Theta < 6.0^\circ$
$np \rightarrow npe^+e^-$	0.463	0.292	0.259
$np \rightarrow \Delta N$	0.146	0.127	0.138
$np \rightarrow \Delta N\pi$	0.104	0.110	0.137
$np \rightarrow np\eta^0$	0.139	0.195	0.211
$np \rightarrow np\rho^0$	0.032	0.032	0.037
$pp \rightarrow \Delta^+p$	0.054	0.066	0.121
$pp \rightarrow \Delta^+N\pi$	0.062	0.178	0.097

from Table 2 that at $M_{ee} > 0.14 \text{ GeV}/c^2$ the main contribution to the dielectron production in the np interaction comes from the channel $np \rightarrow npe^+e^-$, which was calculated in [17]. Fig. 4 presents the momentum distributions of charged particles (protons) calculated within the OPER including the possible channels (see table 1 and Table 2) and their comparison to the HADES data [18]. At the top of Fig. 4, the distributions are presented as functions of the proton momentum p_{FW} registered by the **FW** at $M_{ee} < 140 \text{ MeV}/c$ within three intervals of the angle Θ_{FW} between the proton and the incident deuteron beam. At the bottom of Fig. 4, the same distributions are presented for $M_{ee} > 140 \text{ MeV}/c$. The solid lines in Fig. 4 correspond to our total calculation including the contributions of channels presented in Table 1 and Table 2; the dashed lines are the contributions due to the spectator proton, the dash-dotted curves correspond to the background, which is the contribution of protons produced in the reaction $Np \rightarrow pX$ illustrated by the bottom vertex in Fig. 1. All the results presented in Fig. 4 were obtained including the possible np and pp channels listed in Tables (1,2). Note that the channels $pp \rightarrow pp\pi^0, pp \rightarrow pp\pi^0\pi^0, pp \rightarrow \Delta^+p, pp \rightarrow \Delta^+N\pi$ correspond to the contribution of the spectator neutron. One can see from Fig. 4 that the background contribution is visible in the p_{FW} -spectrum only at large angles $2.0^\circ < \Theta_{FW} < 4.0^\circ$ and it is sizable at $4.0^\circ < \Theta_{FW} < 6.0^\circ$. The description of the HADES data within the OPER and one-baryon exchange (OBE) [19] model is satisfactory except in the region of $4.0^\circ < \Theta_{FW} < 6.0^\circ$ at $M_{ee} > 140 \text{ MeV}$ and at $p_{FW} > 2000 \text{ MeV}/c$, where the error bars are large.

Fig. 5 presents the angular distributions of protons registered by the **FW**. The experimental data were taken from [18]. The dashed line is the contribution of the spectator proton registered by the **FW**, the dash-dotted curve corresponds to the background, which is due to the non spectator protons registered by the **FW**. One

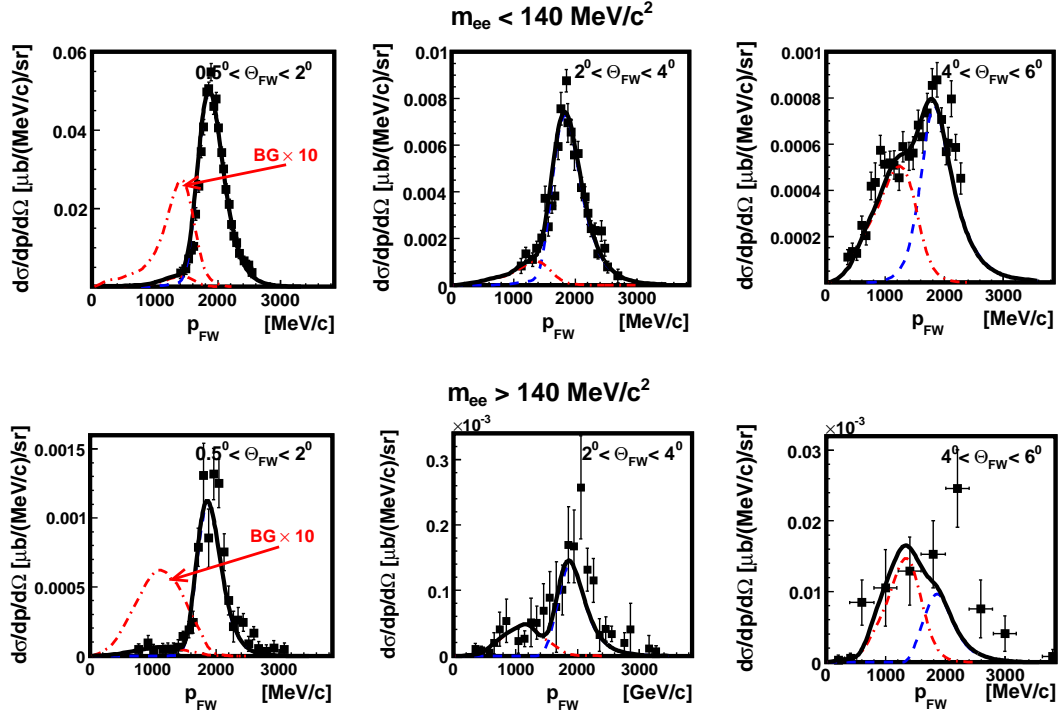


Figure 4: The momentum spectra of protons registered by the **FW** within two ranges of di-electron masses and three ranges of Θ_{FW} . Black squares are experimental data [18], the solid line represents the total description, the dashed curve is the contribution of a true spectator proton, the dash-dotted line corresponds to the background, when the proton produced in reaction $Np \rightarrow pX$ is registered by the **FW**.

can see the description of the HADES data to be satisfactory within the OPER+one-boson exchange (OBE) model. Unfortunately, at $M_{ee} > 140$ MeV/c and $4.0^\circ < \Theta_{FW} < 6.0^\circ$ the statistics is very poor.

Fig. 6 presents the effective mass distribution of e^+e^- -pairs produced in the quasi-free np reaction. To achieve a satisfactory description of the HADES data the following reactions were taken into account [9, 20]:

$$\begin{aligned}
 dp &\rightarrow p_s + (np \rightarrow e^+e^- + X) \\
 &\quad np \rightarrow np\rho^0, (\rho^0 \rightarrow e^+e^-) \\
 &\quad np \rightarrow np\eta^0, (\eta^0 \rightarrow e^+e^- \gamma)
 \end{aligned}$$

The matrix elements squared of the ρ^0 and η^0 Dalitz decays were calculated according to the PLUTO model, see [15, 16]. One can see from Fig. 6 that the main contribution to the M_{ee} spectrum comes from the reaction $np \rightarrow \pi^0 X$ with the subsequent $\pi^0 \rightarrow e^+e^- \gamma$ decay, whereas at large $M_{ee} > 0.3$ GeV/c² the ρ^0 and η meson production in the np interaction contributes significantly and its inclusion allows us to describe the high effective mass behavior of the spectrum. Inclusion of

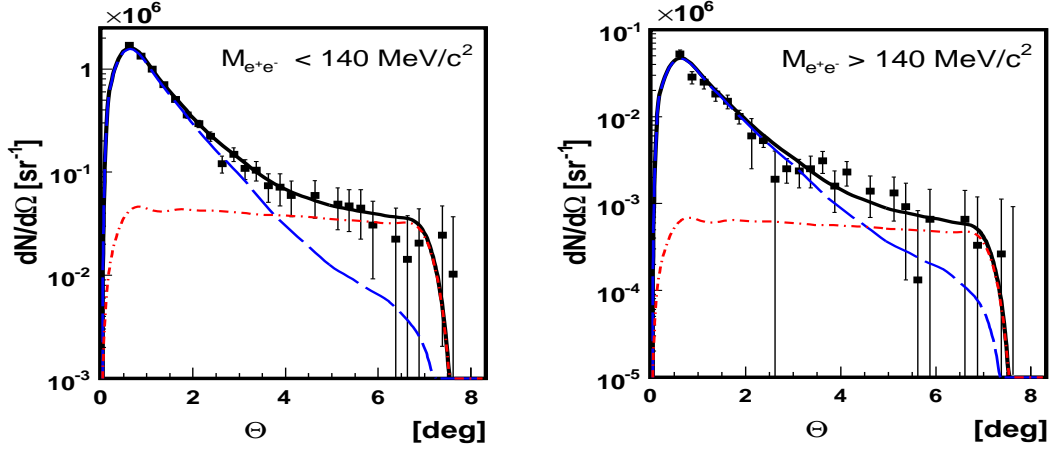


Figure 5: The angular spectra of the charged particles registered at the **FW**. Black squares are the experimental data [18], the solid line is the total description, the dashed line is the contribution of a true spectator proton, the dash-dotted line corresponds to the background, when the proton produced in the reaction $Np \rightarrow pX$ is registered by the **FW**.

the channels listed in Table 1 and Table 2 results in a satisfactory description of the M_{ee} spectrum in the whole kinematical interval, except the very high region of $M_{ee} > 0.6 \text{ GeV}/c^2$. In Fig. 7 the p_T -spectrum of dielectrons is presented for $M_{ee} \leq 0.15 \text{ GeV}/c^2$ (left) and $M_{ee} > 0.15 \text{ GeV}/c^2$ (right). The notation of lines in Fig. 7 is the same as in Fig. 6. One can see from Fig. 7 that inclusion of the contributions of the np channels mentioned above allows us to describe the transverse momentum spectrum of dielectrons more or less satisfactorily at $p_T \leq 0.4 \text{ GeV}/c$.

3. Conclusion

The successful description of the proton spectra in FW (PFW) of HADES was obtained by taking into account the various np reactions and pp processes, as a background.

The reaction $np \rightarrow np\pi^0 \rightarrow npe^+e^-\gamma$ provides the main contribution to the spectator momentum spectra at small dielectron effective masses $M_{ee} < 140 \text{ MeV}/c$. The reaction $np \rightarrow npe^+e^-$ results in a significant contribution at $M_{ee} > 140 \text{ MeV}/c^2$ and $0.5^\circ < \Theta_{p,FW} < 6^\circ$ as compared to other channels.

At larger angles ($2.0^\circ < \Theta_{p,FW} < 4^\circ$) and PFW $< 2000 \text{ MeV}/c$, one should also take into account the spectator neutron case as well as $pp \rightarrow e^+e^- + X$ reactions.

For a satisfactory description of the M_{ee} spectrum it is also necessary to take into account the reactions $np \rightarrow np\eta^0$ and $np \rightarrow np\rho^0$ with subsequent decays ($\eta^0 \rightarrow e^+e^-\gamma$ and $\rho^0 \rightarrow e^+e^-$ respectively) in addition to the reaction used for the description of PFW spectra.

quasi-free n+p 1.25 GeV

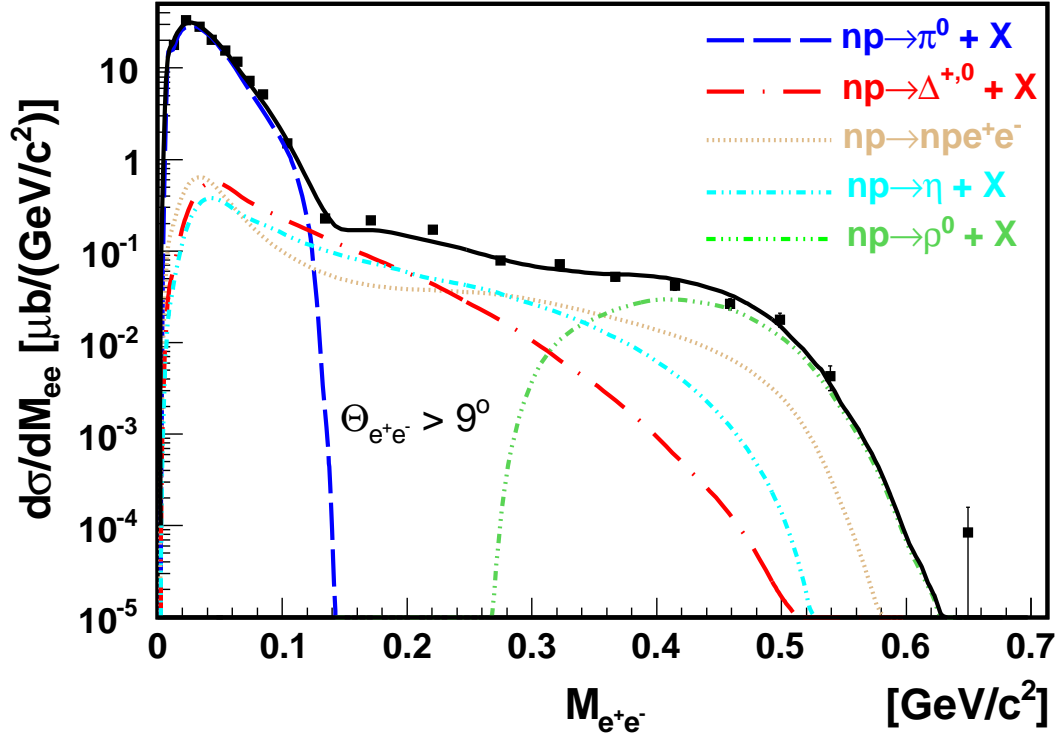


Figure 6: The effective mass spectrum of e^+e^- -pairs. The black squares represent experimental the smooth curves result from calculations using the (OPER+OBE)-model involving the contributions of different np channels.

Acknowledgements. The authors are grateful to members of the HADES Collaboration P.Salabura, J.Stroth, R.Holzmann, T.Galatyuk, G.Kornakov, V.P.Ladygin, K. Lapidus, A.I.Malakhov, A.Rustamov, V.Pechenov for very useful discussions, which stimulated us to do this analysis.

References

- [1] P.D.B Collins P.D.B. An Introduction to Regge Theory and High Energy Physics. Cambridge University Press, (1977).
- [2] L.A. Ponomarev, *Sov.J.Part.Nucl.* **7**, 70 (1976).
- [3] A.P.Jerusalimov et al., *Eur.Phys.J. A* **51**, 83 (2015).

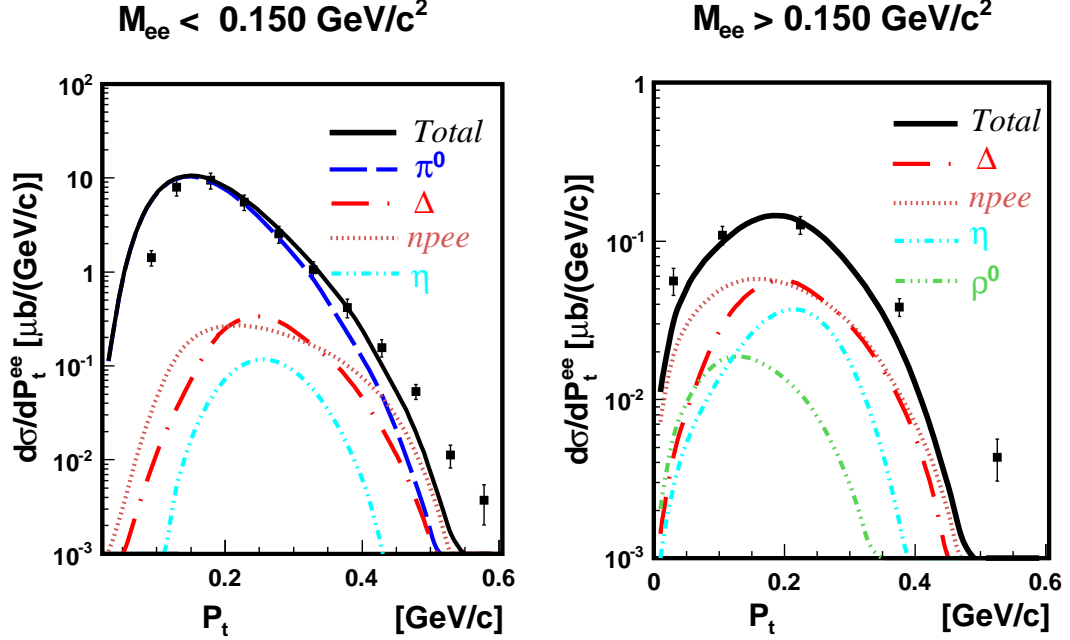


Figure 7: Left: the p_T distribution of dielectrons at $M_{ee} \leq 0.15 \text{ GeV}/c^2$. Right: the same distribution at $M_{ee} > 0.15 \text{ GeV}/c^2$. The black squares are experimental data [20]. The solid line is our total calculation involving all the np channels mentioned in Table 1 and Table 2.

- [4] G. Agakishiev et al.[HADES Collaboration], *Phys.Lett. B* **750**, 184 (2015). arXiv:1503.04013v2.
- [5] A.P. Jerusalemov, arXiv:1203.3330[nucl-th] (2012).
- [6] A.P. Jerusalemov, arXiv:1208.3982[nucl-th] (2012).
- [7] A.P. Jerusalemov, PoS BaldinISHEPPXXII, 048 (2015).
- [8] G. Agakishiev et al.[HADES Collaboration], *Eur.Phys.J. A* **41**, 243 (2009).
- [9] K. Lapidus et al. arXiv:0904.1128 [nucl-ex] (2009).
- [10] O.V.Andreeva, et al., *Instrum.Exp.Techn.*, **57**, 103 (2014).
- [11] R.Machleidt, et al., *Phys.Rev.C* **63**, 024001 (2001).
- [12] A.N.Kamalov and L.A.Ponomarev, *Sov. J. Nucl. Phys.*, **23**, 566 (1976).
- [13] G.V. Beketov et al., *Sov. J. Nucl. Phys.* **29**, 201 (1979). [arXiv:0905.2568 [nucl-ex]].
- [14] L.G. Landsberg, *Phys.Rept.* **128**, 301 (1985).

- [15] I. Frohlich, T. Galatyuk, R. Holzmann, J. Markert, B. Ramstein, P. Salabura and J. Stroth, *J.Phys.Conf. Ser.* **219**, 032039 (2010).
- [16] I. Frohlich, et al., arXiv:0708.2382 [nucl-ex] (2007).
- [17] A.P. Jerusalemov and G.I. Lykasov *Int. J. Mod. Phys. Conf. Ser.*, **39**, 1560111 (2015)
- [18] K. Lapidus, Production of electron-positron pairs in quasi-free n-p collisions. PhD thesis, Institute of Nuclear Research RAS, Moscow, 2010.
- [19] A.B. Kaidalov and A.F. Nilov, *Sov.J.Nucl.Phys.* **41**, 490 (1985);
Sov.J.Nucl.Phys. **52**, 1060 (1990).
- [20] T.Galatyuk. PhD thesis "Di-electron spectroscopy in HADES and CBM: from $p + p$ and $n + p$ collisions at GSI to $Au + Au$ collisions at FAIR", Johann Wolfgang Goethe-Universitaet, <http://nbn-resolving.de/urn/resolver.pl?urn:nbn:de:hebis:30-71896>.